Deep UV resonant Raman spectroscopy for photodamage characterization in cells

Yasuaki Kumamoto,[1,2] Atsushi Taguchi,[2] Nicholas Isaac Smith,[3] and Satoshi Kawata[1,2,*]

[1]*Department of Applied Physics, Graduate School of Engineering, 2-1 Yamadaoka, Suita, Osaka 565-0871, Japan*
[2]*Nanophotonics Laboratory, RIKEN Advanced Science Institute, 2-1 Hirosawa, Wako Saitama 351-0198, Japan*
[3]*Biophotonics Laboratory, Immunology Frontier Research Center, Osaka University, 2-1 Yamadaoka, Suita, Osaka 565-0871, Japan*
**kawata@ap.eng.osaka-u.ac.jp*

Abstract: We employed deep UV (DUV) Raman spectroscopy for characterization of molecular photodamage in cells. 244 nm light excitation Raman spectra were measured for HeLa cells exposed to the excitation light for different durations. In the spectra obtained with the shortest exposure duration (0.25 sec at 16 $\mu W/\mu m^2$ irradiation), characteristic resonant Raman bands of adenine and guanine at 1483 cm^{-1} and tryptophan and tyrosine at 1618 cm^{-1} were clearly visible. With increasing exposure duration (up to 12.5 sec), these biomolecular Raman bands diminished, while a photoproduct Raman band at 1611 cm^{-1} grew. By exponential function fitting analyses, intensities of these characteristic three bands were correlated with sample exposure duration at different intensities of excitation light. We then suggest practical excitation conditions effective for DUV Raman observation of cells without photodamage-related spectral distortion.

OCIS codes: (300.6450) Spectroscopy, Raman; (300.6540) Spectroscopy, ultraviolet; (350.1820) Damage; (170.1530) Cell analysis; (170.5660) Raman spectroscopy.

References and links

1. S. Nocentini and L. Chinsky, "In vivo studies of nucleic acid by ultraviolet resonance Raman spectroscopy on eucaryotic living cells," J. Raman Spectrosc. **14**(1), 9–10 (1983).
2. Y. Yazdi, N. Ramanujam, R. Lotan, M. F. Mitchell, W. Hittelman, and R. Richards-Kortum, "Resonance Raman spectroscopy at 257 nm excitation of normal and malignant cultured breast and cervical cells," Appl. Spectrosc. **53**(1), 82–85 (1999).
3. U. Neugebauer, U. Schmid, K. Baumann, W. Ziebuhr, S. Kozitskaya, V. Deckert, M. Schmitt, and J. Popp, "Towards a detailed understanding of bacterial metabolism--spectroscopic characterization of *Staphylococcus epidermidis*," ChemPhysChem **8**(1), 124–137 (2007).
4. P. V. Zinin, A. Misra, L. Kamemoto, Q. Yu, N. Hu, and S. K. Sharma, "Visible, near-infrared, and ultraviolet laser-excited Raman spectroscopy of themonocytes/macrophages (U937) cells," J. Raman. Spectrosc. **41**, 268–274 (2010).
5. R. Manoharan, E. Ghiamati, R. A. Dalterio, K. A. Britton, W. H. Nelson, and J. F. Sperry, "UV resonance Raman spectra of bacteria, bacterial spores, protoplasts and calcium dipicolinate," J. Microbiol. Methods **11**(1), 1–15 (1990).
6. S. Kaminaka, Y. Imamura, M. Shingu, T. Kitagawa, and T. Toyoda, "Studies of bovine enterovirus structure by ultraviolet resonance Raman spectroscopy," J. Virol. Methods **77**(2), 117–123 (1999).
7. Q. Wu, T. Hamilton, W. H. Nelson, S. Elliott, J. F. Sperry, and M. Wu, "UV Raman spectral intensities of *E. coli* and other bacteria excited at 228.9, 244.0, and 248.2 nm," Anal. Chem. **73**(14), 3432–3440 (2001).
8. M. Baek, W. H. Nelson, D. Britt, and J. F. Sperry, "UV-excited resonance Raman spectra of heat denatured lysozyme and staphylococcus epidermidis," Appl. Spectrosc. **42**(7), 1312–1314 (1988).
9. M. Schmitt and J. Popp, "Raman spectroscopy at the beginning of the twenty-first century," J. Raman Spectrosc. **37**(1-3), 20–28 (2006).
10. M. Harz, M. Krause, T. Bartels, K. Cramer, P. Rösch, and J. Popp, "Minimal invasive gender determination of birds by means of UV-resonance Raman spectroscopy," Anal. Chem. **80**(4), 1080–1086 (2008).
11. W. F. Vincent and P. J. Neale, *Mechanisms of UV Damage to Aquatic Organisms* (Cambridge University Press: Cambridge, 2000), Chap 6.
12. H. Görner, "Photochemistry of DNA and related biomolecules: quantum yields and consequences of photoionization," J. Photochem. Photobiol. B **26**(2), 117–139 (1994).
13. J.-L. Ravanat, T. Douki, and J. Cadet, "Direct and indirect effects of UV radiation on DNA and its components," J. Photochem. Photobiol. B **63**(1-3), 88–102 (2001).
14. M. Harz, R. A. Claus, C. L. Bockmeyer, M. Baum, P. Rösch, K. Kentouche, H.-P. Deigner, and J. Popp, "UV-resonance Raman spectroscopic study of human plasma of healthy donors and patients with thrombotic microangiopathy," Biopolymers **82**(4), 317–324 (2006).

#138099 - $15.00 USD Rec. 12 Nov 2010; revised 18 Feb 2011; accepted 9 Mar 2011; published 18 Mar 2011

15. F. Sureau, L. Chinsky, C. Amirand, J. P. Ballini, M. Duquesne, A. Laigle, P. Y. Turpin, and P. Vigny, "An ultraviolet micro-Raman spectrometer: resonance Raman spectroscopy within single living cells," Appl. Spectrosc. **44**(6), 1047–1051 (1990).
16. V. Pajcini, C. H. Munro, R. W. Bormett, R. E. Witkowski, and S. A. Asher, "UV Raman microspectroscopy: spectral and spatial selectivity with sensitivity and simplicity," Appl. Spectrosc. **51**(1), 81–86 (1997).
17. Q. Wu, G. Balakrishnan, A. Pevsner, and T. G. Spiro, "Histidine photodegradation during UV resonance Raman spectroscopy," J. Phys. Chem. A **107**(40), 8047–8051 (2003).
18. K. Lao and A. N. Glazer, "Ultraviolet-B photodestruction of a light-harvesting complex," Proc. Natl. Acad. Sci. U.S.A. **93**(11), 5258–5263 (1996).
19. C. R. Johnson, M. Ludwig, and S. A. Asher, "Ultraviolet resonance Raman characterization of photochemical transients of phenol, tyrosine, and tryptophan," J. Am. Chem. Soc. **108**(5), 905–912 (1986).
20. M. P. Russell, S. Vohník, and G. J. Thomas, Jr., "Design and performance of an ultraviolet resonance Raman spectrometer for proteins and nucleic acids," Biophys. J. **68**(4), 1607–1612 (1995).
21. M. M. Mariani, P. Lampen, J. Popp, B. R. Wood, and V. Deckert, "Impact of fixation on in vitro cell culture lines monitored with Raman spectroscopy," Analyst (Lond.) **134**(6), 1154–1161 (2009).
22. S. Iwanaga, N. I. Smith, K. Fujita, and S. Kawata, "Slow $Ca^{(2+)}$ wave stimulation using low repetition rate femtosecond pulsed irradiation," Opt. Express **14**(2), 717–725 (2006).
23. A. C. Ferrari and J. Robertson, "Resonant Raman spectroscopy of disordered, amorphous, and diamondlike carbon," Phys. Rev. B **64**(7), 075414 (2001).
24. D. Voet, W. B. Gratzer, R. A. Cox, and P. Doty, "Absorption spectra of nucleotides, polynucleotides, and nucleic acids," Biopolymers **1**(3), 193–208 (1963).
25. H. C. Bolton and J. J. Weiss, "Hypochromism in the ultra-violet absorption of nucleic acids and related structures," Nature **195**(4842), 666–668 (1962).
26. S. Roy, *Strategies for the Minimisation of UV-Induced Damage* (Cambridge University Press: Cambridge, 2000), Chap. 7.

1. Introduction

Deep UV (DUV) Raman spectroscopy selectively visualizes nucleotide bases and aromatic amino acids in cells due to the resonant effect [1–8]. In the resonant Raman condition, where the electronic transition energy of a molecule corresponds to photon energy of Raman excitation light, the Raman scattering intensity of the molecule is enhanced by as much as 10^6 compared to the non-resonant Raman scattering [9]. Because other biological compounds in cells, such as lipids and sugars, are not in the resonant condition at DUV, Raman scattering from nucleotide bases [1–7] and aromatic amino acids [1–8] are selectively enhanced in DUV resonant Raman spectroscopy of cells.

In DUV Raman spectroscopy of cells, molecular photodegradation often occurs during the measurement [10]. The photodamage of biomolecules is caused via strong absorption. The photon energy of DUV is sufficiently high for excited molecules to be broken or react with surrounding media [11–13]. Particularly, the accompanying photodamage is a serious issue for observation of biomolecules in a small volume [14]. This makes it difficult to achieve microscopic observation of living cells with high spatial resolution [15,16]. It is then important to understand the molecular degradation in cells during DUV Raman measurement, and to be aware of the light intensities and exposure times which bring about such effects.

DUV-induced molecular degradation in whole cells has not previously been characterized. Degradation [17,18] or phototransient states [19] of some individual biomolecules have been characterized by using DUV Raman spectroscopy, but individual molecules don't accurately represent the photodamage that occurs in whole cells. Molecular level analyses of the ensemble of molecules are required for useful characterization of photodamage in whole cells.

In this study, we employed DUV resonant Raman spectroscopy for direct characterization of the accompanying molecular degradation in cells. The characteristic resonant Raman bands of nucleotide bases and aromatic amino acids were analyzed in the DUV Raman spectra of HeLa cells exposed to excitation light for different durations at different intensities. The intensity of characteristic Raman bands were correlated with the exposure durations at different excitation intensities. In the obtained spectra, we identified the growth of a photoproduct band. The growth of the photoproduct band was also correlated with the exposure durations of excitation light at different intensities. This study will suggest an exposure condition effective for practical use of DUV resonant Raman spectroscopy of cells without spectral distortion as well serve to provide quantitative understanding of the Raman spectra of cells, which are often composed of both intact sample signals and photoproduct noise.

#138099 - $15.00 USD Rec. 12 Nov 2010; revised 18 Feb 2011; accepted 9 Mar 2011; published 18 Mar 2011

2. Materials and methods

2.1. Deep UV Raman spectroscopy

A purpose-built Raman microscope was used for the experiments. The 244 nm continuous oscillation line of an Argon ion SHG laser (Coherent Innova 300C MoToFRED) was used as the Raman excitation light. 244 nm is the wavelength optimized to resonantly excite both nucleotides and aromatic amino acids. The laser intensity is controlled by an ND filter. The expanded and collimated beam was introduced into a 40x UV achromatic objective lens (OFR LMU-40x UVB, NA = 0.5) equipped on a Nikon inverted microscope via non-polarized beam splitter. The beam was focused at the interface between the sample and the substrate. The area of focus was estimated to be ~1 μm^2. The scattering light was collected by the same objective with back scattering geometry. Rayleigh scattering light was rejected by longwave-pass edge filter having an optical density of 4.0. The transmitted light was guided into a spectrometer and dispersed by a 3600 G/mm grating. Raman spectra were measured using a back-illuminated cooled-CCD (Princeton Instruments SPEC-10 2KBUV). The grating dispersion was calibrated using the excitation wavelength, and the Raman bands of sulfate ion (981 cm^{-1}) and acetonitrile (2249 cm^{-1}) [20]. All Raman measurements were done at room temperature.

Raman spectra were measured at different sample exposure durations. For a fair spectral comparison among different sample exposure durations, we measured the same sample area repeatedly with a constant spectral acquisition time and then observed how the spectra changed with accumulating exposure. Each spectrum was obtained by integrating the spectral signal on the detector over a large number (200) of micro-observation positions in order to obtain sufficient S/N for quantitatively analyzing slight changes in cell spectra. Measurement points were separated from each other in space by 5 μm, a distance 5 times larger than the focal spot diameter. Since the output spectrum was accumulated from 200 positions, the final data structure is just one spectrum for each exposure time. The entire measurements were then repeated 3 times to provide a measure of repeatability. The standard deviations shown in Figs. 1, 2 and 3 are therefore calculated from the deviations between the three output spectra for the same conditions.

2.2. Samples

HeLa cells were purchased from Genlantis, Inc. The cells were cultured on quartz substrates with Dulbecco's modified Eagled medium for 2~4 days in a 5% CO_2 incubator at 37 degrees and 100% humidity. The cells were used at the confluent density.

Different treatments were performed on cultured cells according to the purpose of the Raman measurements. For experiments done to quantitatively correlate the molecular degradations with the exposure durations and intensities, desiccated cells were used, because desiccated cells are not affected by diffusion of molecules. The desiccation treatment of the cells was performed according to the literature [21]. Briefly, the procedure was to rinse the cells with Tyrode's solution, then the cells were placed in a desiccator containing silica gel beads for 1 hour under ambient pressure. Following treatment, all samples were wrapped in aluminum foil and stored at –20 degree until analysis. The desiccation treatment is claimed to best preserve cell components and their Raman spectra, even though it may cause autolysis [21].

Live cells were also analyzed in order to understand photodamage in live cells and its effect on Raman spectra. Although Raman spectra of live cells can't exactly be correlated with exposure energy due to the molecular diffusion, it is possible to evaluate quantities of the spectra. Live cells were rinsed and replaced with Tyrode's solution in advance of Raman measurement.

Live cells with exogenous antioxidant agents were also analyzed in order to understand the effect of reactive oxygen species on Raman spectra and to determine whether they could moderate the photodegradation process. 6-hydroxy-2,5,7,8-tetramethyl-chroman-2-carboxylic acid (Trade name: Trolox) was used as an antioxidant agent. Trolox is a model compound of water-soluble and plasma-membrane-permeable antioxidant agent [22]. For these experiments, live cells were placed in Tyrode's solution with a concentration of 500 μM Trolox 30 min in advance of Raman measurements.

#138099 - $15.00 USD Rec. 12 Nov 2010; revised 18 Feb 2011; accepted 9 Mar 2011; published 18 Mar 2011

Additionally, fixed cells were analyzed in order to compare living and non-living cell samples in liquid bath media to determine the effect of cellular function on the resulting Raman spectra. For these experiments, the cells were fixed with paraformaldehyde. Live cells were rinsed by PBS before fixation, then placed in PBS solution at concentration of 2% paraformaldehyde for 20 min. After fixation, the cells were rinsed and immersed with Tyrode's buffer solution.

2.3. Evaluation of Raman band intensity

To evaluate the Raman band intensity, each Raman band was first reproduced by single- or multi-component Lorentzian function with a linearly tilting baseline.

$$MultiLor(x) = y_0 + ax + \sum_{i=1}^{n} \frac{b_i}{(x - x_i)^2 + \sigma_i^2} \tag{1}$$

All constants (a, b_i, σ_i, y_0, and x_i) are obtained from the fitting process (i = 1,2,…,n; 'n' is the number of fitting bands). Then, the Raman band intensity was defined as the integral of a Lorentzian part of Eq. (1), that is, obtained by Eq. (2).

$$I = \int_{-\infty}^{\infty} \frac{b_i}{(x - x_i)^2 + \sigma_i^2} dx \tag{2}$$

All fitting processes were performed on Igor 6.05A.

2.4. Exponential function fitting for Raman band intensity

The change in Raman band intensity is expected to correlate with a change in the number of observable molecules, therefore is represented by a rate equation. A solution of the equation is exponential decay or cumulative function.

$$F(t) = y_0 + \sum_{i=1}^{m} A_i \exp\left(-\frac{t}{\tau_i}\right) \tag{3}$$

τ_i (i = 1,2,...,m. m: the number of fitting components) is a time constant. y_0 and A_i are constants. A_i is positive for a decay component, while A_i will be negative for any component that cumulatively rises. The fitting procedure by using Eq. (3) was applied to the temporal change in Raman band intensity. The curve fitting procedures were performed on Igor 6.05A.

3. Results and discussion

3.1. Change in spectra of cells depending on duration of DUV exposure

Figure 1(a) shows the obtained Raman spectra of desiccated HeLa cells with accumulating exposure durations. Each Raman spectrum was obtained with different durations (0.250, 0.500, 1.00, 2.50, 5.00, 7.50, 10.0, 12.5 sec) of sample exposure to the excitation light at 16 $\mu W/\mu m^2$ irradiation. In the spectrum obtained for the exposure duration of 0.250 sec, several characteristic spectral peaks are observed. Table 1 shows assignments of those characteristic peaks observed in the spectrum. All peaks are assigned to one or more nucleotide bases and aromatic amino acids [3,4]. As the exposure duration increases (up to 12.5 sec), the characteristic bands decay. In the spectrum obtained for the exposure duration of 12.5 sec, the characteristic bands of nucleotide bases and aromatic amino acids are barely visible, while two broad bands are observed at approximately 1380 and 1610 cm^{-1}. Similar spectra have been reported as spectra of polymeric hydrogenated amorphous carbon [23]. Polymeric hydrogenated amorphous carbon shows two characteristic bands as D and G peaks at approximately 1400 and 1600 cm^{-1}, respectively, with a spectral dip at approximately 1500 cm^{-1}. This indicates that the photoproduct Raman bands observed in photodegraded cells may be assigned to polymeric amorphous carbon. We also measured the same characteristics for photodegraded albumin (one of the model proteins), but not for the others (nucleotide bases and lipids). The results suggest that proteins in cells were degraded into polymeric hydrogenated amorphous carbon in DUV Raman observation.

#138099 - $15.00 USD Rec. 12 Nov 2010; revised 18 Feb 2011; accepted 9 Mar 2011; published 18 Mar 2011

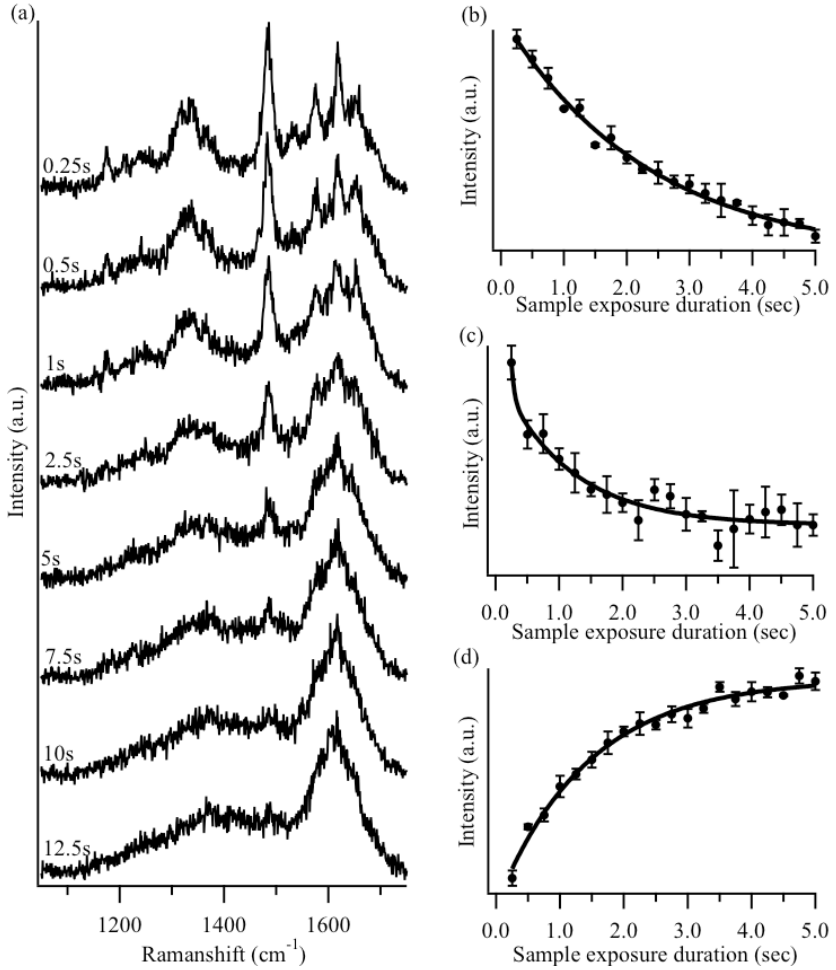

Fig. 1. (a) Raman spectra of desiccated cells obtained at different durations of sample exposure (0.25, 0.5, 1, 2.5, 5, 7.5, 10, 12.5 sec) at 16 μW/μm^2 irradiation. Each spectrum is shifted vertically for clear comparison. (b-d) shows the intensity of Raman band at (b) 1483, (c) 1618, and (d) 1611 cm^{-1} plotted over sample exposure duration, and their corresponding fitting curves. Each spectrum was built-up from 200 different sample positions, with the signal accumulated at the detector. This was repeated 3 times and the error bars were set to the standard deviations between the 3 measurements.

Table 1. Raman band assignments for DUV Raman spectrum of an intact cellular sample[a]

Raman shift (cm^{-1})	1003	1178	1211	1240 1336	1358	1483	1529	1575	1618	1652
Assignment	Trp	Tyr	Tyr	G A Tyr U	T A	A G	C	G A	Trp Tyr	T

[a]Refer to [3,4]. The abbreviations; A: adenine, G: guanine, T: thymine, C: cytosine, U: uracil, Tyr: tyrosine, Trp: tryptophan.

Now we focus on the exposure duration dependence of three characteristic Raman bands at 1483 cm^{-1} (adenine and guanine), 1618 cm^{-1} (tryptophan and tyrosine), and 1611 cm^{-1} (photoproduct). The intensity of these Raman bands is plotted against the sample exposure duration, as shown in Fig. 1(b-d). The plots can clearly visualize the relationship of the Raman band intensity and the sample exposure duration. Figure 1(b, and c) clearly prove the Raman band intensities of purine bases and aromatic amino acids exponentially decrease as the sample exposure duration increases up to 12.5 sec. Figure 1(d) shows that the intensity of photoproduct Raman band cumulatively increases with an increase in the exposure duration.

#138099 - $15.00 USD Rec. 12 Nov 2010; revised 18 Feb 2011; accepted 9 Mar 2011; published 18 Mar 2011

In order to quantify the relationship between the Raman band intensity and sample exposure duration, we applied procedures of exponential function fitting to the intensity plots. The Raman band of purine bases at 1483 cm^{-1} was best fit by the exponential decay function with a single time constant. The resulting time constant of $\tau_1 = 2.3$ was obtained. The fitting curve is shown also in Fig. 1(b). It is interesting that the degradation of two purine bases is reproduced by a single component. The chemical structure is very similar for adenine and guanine, and their absorbance at 244 nm is close [24]. The adenine and guanine time profiles may represent similar reactions with excitation photons. For the photoproduct band at 1611 cm^{-1}, the curve was best fit by the exponential cumulative function with a single time constant of $\tau_1 = 1.4$ as also shown in Fig. 1 (d). Though the formation of amorphous carbon photoproduct should be derived from complex pathways, there must be a single essential pathway that dominates the growth of the photoproduct. In contrast from the other two components, the aromatic amino acid band at 1618 cm^{-1} was best fitted by an exponential decay function with two time constants. The fitting curve is also shown in Fig. 1(c). The resultant time constants of $(\tau_1, \tau_2) = (1.1, 0.048)$ were obtained. The decay of the aromatic amino acid band showed a fast initial decay followed by a slower decrease in intensity. Each time constant can be assigned to the degradation of tyrosine and tryptophan. Because tyrosine and tryptophan have totally different chemical structure, the Raman band plot was represented by two components. We also notice that the growth of photoproduct is slower than the decays of aromatic amino acids, but faster than the decay of purine bases. It is conceivable, although difficult to prove, that at least one of the decay components in the aromatic amino acid band contributes for to the rise in photoproducts. This notion is consistent with the previous discussion that the photoproducts originate from proteins.

The degree of molecular degradation could depend on the intensity of Raman excitation light, since the photodamage would be related to molecular phototransient states [19], heating, and/or multiphoton absorption processes [12,18]. We compared the molecular degradation among different Raman excitation intensities of 1.6, 4.0, 8.0, and 16 $\mu W/\mu m^2$. Figure 2(a) shows Raman spectra obtained at 1.6 $\mu W/\mu m^2$ irradiation for different durations (2.50, 5.00, 10.0, 25.0, 50.0, 75.0, 100, 125 sec) of the sample exposure. Similarly to the case of 16 $\mu W/\mu m^2$ irradiation, the Raman intensities of aromatic amino acids and nucleotide bases bands diminished, while the photoproduct band rose, as the sample exposure duration increases (up to 125 sec). Figure 2(b-d) shows plots of the intensity of the same three characteristic Raman bands at 1483, 1618, and 1611 cm^{-1}, and their fitting curves. The intensity plot of 1483 cm^{-1} purine bases band, 1618 cm^{-1} aromatic amino acids band, and 1611 cm^{-1} photoproduct bands are fitted by a single time constant exponential decay function, two time constant exponential decay function, and a single time constant exponential cumulative function, respectively. The fitting methods and number of time constants were the same as that for 16 $\mu W/\mu m^2$. The same relationships between Raman spectra of the cells and the sample exposure durations were also observed at 4.0 and 8.0 $\mu W/\mu m^2$ irradiation.

For a comparison of the molecular degradation among different irradiation intensities, it is helpful to compare the obtained time constants of fitting curves. The time constants are summarized in Table 2. For the purine bases and photoproduct, the time constants are inversely proportional to the irradiation intensity. This is a strong indication of the fact that the number of exposure photons determines the amount of destruction of the purine bases and the growth of photoproduct regardless of the excitation irradiation intensity. This implies that the photodegradation of purine bases and the growth of photoproduct is not associated with heating, molecular phototransients, and multi-photon absorption process in the current measurement conditions. For the aromatic amino acids band, though the relationship between the time constants and irradiation intensity is also close to inversely proportional, the contributions of faster and slower components are different at different irradiation intensities. The aromatic amino acids band obtained at 16 and 8.0 $\mu W/\mu m^2$ irradiations is mainly composed of the faster decay component, while for 1.6 and 4.0 $\mu W/\mu m^2$ the slower component is dominant. This indicates that the degradation of aromatic amino acids is nonlinearly dependent on the irradiation intensity and can be associated with time-dependent effects such as heating, molecular phototransients, and multi-photon absorption process.

#138099 - $15.00 USD Rec. 12 Nov 2010; revised 18 Feb 2011; accepted 9 Mar 2011; published 18 Mar 2011

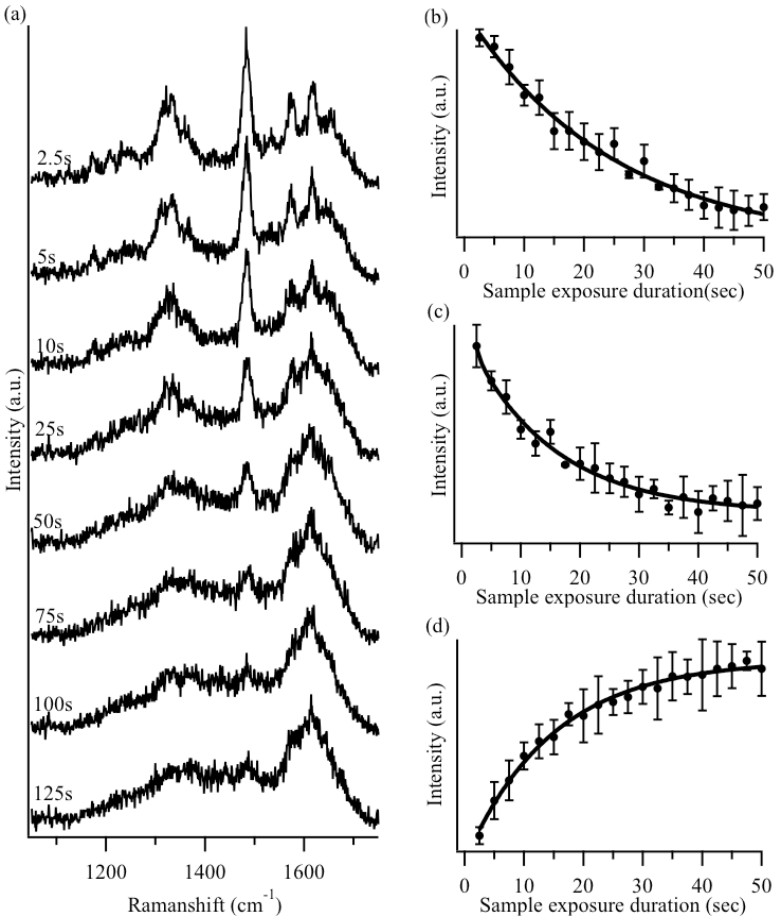

Fig. 2. (a) Raman spectra of desiccated cells obtained at different durations of sample exposure (2.5, 5, 10, 25, 50, 75, 100, 125 sec) at 1.6 μW/μm^2 irradiation. Each spectrum is shifted vertically for clear comparison. (b-d) shows the intensity of the Raman band at (b) 1483, (c) 1618, and (d) 1611 cm^{-1} plotted on sample exposure duration, and their fitting curves. The error bars were assigned in the same manner as for Fig. 1.

Table 2. Time constants obtained by the curve fitting

Irradiation intensity (μW/μm^2)	Time constant			
	Purine (1483 cm^{-1})	Aromatic amino acid* (1618 cm^{-1})		Photoproduct (1611 cm^{-1})
16	2.3	1.1(0.41)	0.048 (0.59)	1.4
8.0	5.1	3.3 (0.38)	0.11 (0.62)	2.3
4.0	9.8	6.2 (0.54)	0.38 (0.46)	5.5
1.6	25	14 (0.8)	0.58 (0.2)	15

*In parentheses, the contribution of the component to the fitting curve is shown.

The obtained Raman spectra also contain contributions from thymine. An interesting result was observed for the exposure duration dependence of the intensity of the thymine Raman band at 1652 cm^{-1}. The intensity plot for 1652 cm^{-1} thymine band is shown in Fig. 3. Interestingly, the intensity change shows the transient increase during short exposures (up to 0.75 sec), followed by a monotonic decrease over exposures longer than 0.75 sec. The characteristics of transient increase were observed for all different irradiation intensities of 1.6, 4.0, 8.0, and 16 μW/μm^2. The temporal behavior of the thymine band intensity is not clearly understood, but the possible explanation of transient increase can be either generation of transient photoproduct molecules, which show a band at the same wavenumber or the scattering efficiency increase due to the breakdown of hypochromism,

#138099 - $15.00 USD Rec. 12 Nov 2010; revised 18 Feb 2011; accepted 9 Mar 2011; published 18 Mar 2011

which is known as a phenomenon where the absorbance of nucleotide bases becomes lower when they are stacked in DNA structure [25]. Base releases from DNA can occur by DUV irradiation [12], resulting in the disappearance of hypochromism.

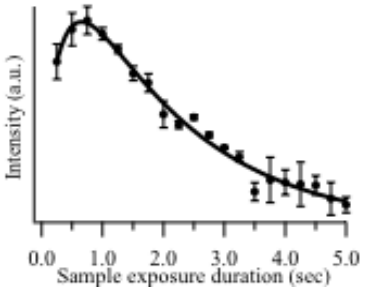

Fig. 3. The intensity of the thymine band at 1652 cm^{-1} plotted on sample exposure duration for 1.6 $\mu W/\mu m^2$ irradiation and its fitting curve. The error bars were assigned in the same manner as for Fig. 1.

3.2. Estimation of effective or allowable maximum exposure energy

The obtained fitting functions correlate the exposure duration and intensity with the Raman band intensities. From the fitting curves, it is now possible to suggest a practically effective maximum energy of Raman excitation light for DUV Raman observation of cells. In terms of observation of biomolecules in cells, it is reasonable to say that the effective maximum energy can be considered to be the exposure energy where the Raman band intensity drops to 1/e of the intact cell signal. For a single-component exponential decay function, the product of irradiation intensity and time constant for the fit curve gives this exposure energy. It must be noted that values of an exponential decay function become negligibly small with times larger than the time constant. This means that exposure larger than the effective maximum energy just increases molecular damage in the DUV Raman observation. For a multiple-component exponential decay function, the same criterion can be used to derive the practically effective maximum energy.

The effective maximum energies for purine bases and aromatic amino acids at different irradiation intensities are shown in Table 3. Regardless of irradiation intensity, the appropriate maximum energy for observing purine bases is similar (37- 41 $\mu J/\mu m^2$). For Raman band of aromatic amino acids (1618 cm^{-1}), on the other hand, the effective maximum energy decreases by an order of magnitude with an increase of irradiation intensity from 1.6 to 16 $\mu W/\mu m^2$. It is concluded that observation of aromatic amino acids must be done with smaller exposure energy for suppressing the effects of photodanage, while the observation of purine bases doesn't require the tuning of the excitation light intensity.

Table 3. Effective or allowable maximum energy of excitation light exposure

Irradiation intensity ($\mu W/\mu m^2$)	Exposure energy ($\mu J/\mu m^2$)		
	Purine (1483 cm^{-1})	Aromatic amino acid (1618 cm^{-1})	Photoproduct (1611 cm^{-1})
16	37	1.8	22
8.0	41	2.8	18
4.0	39	9.6	22
1.6	40	18	24

It is also important to note the practically allowable maximum exposure energy for suppressing the growth of photoproduct in the Raman spectra. The allowable maximum exposure energy may be obtained using similar criterion to the effective maximum exposure energy for observation of biomolecules, and be considered as the exposure energy where the Raman band intensity rises to (1-1/e) of saturated photoproduct intensity. For an exponential cumulative function, the area of the function below this defined energy threshold is negligibly small. Thus the practically allowable maximum energy was obtained as the product of irradiation intensity and time constant. According

#138099 - $15.00 USD Rec. 12 Nov 2010; revised 18 Feb 2011; accepted 9 Mar 2011; published 18 Mar 2011

to Table 3, the practically allowable maximum energy in terms of limiting the growth of photoproduct is therefore in the range between 18 and 24 μJ/μm^2. There is little dependence of the allowable energy on the excitation intensity.

3.3. Qualitative evaluation of photodamage on live cells

Understanding photodamage of live cells is also important, though quantification of the molecular degradation is difficult due to molecular diffusion during exposure. Qualitative characteristics of Raman spectra from live cells were then analyzed. Figure 4 shows the Raman spectra of live cells obtained for different durations (5, 10, 15 sec) of sample exposure to 16 μW/μm^2 excitation light. The spectra obtained at the exposure duration of 15 s barely show the Raman band of purine bases at approximately 1480 cm^{-1}, while the photoproduct bands at approximately 1380 and 1610 cm^{-1} are dominantly visible. These spectral characteristics are the same as observed in desiccated cells. Therefore, it is concluded that the quantities of photodamage of live cells are essentially the same as in the case of desiccated cells, although it is hard to precisely quantify the photodamage.

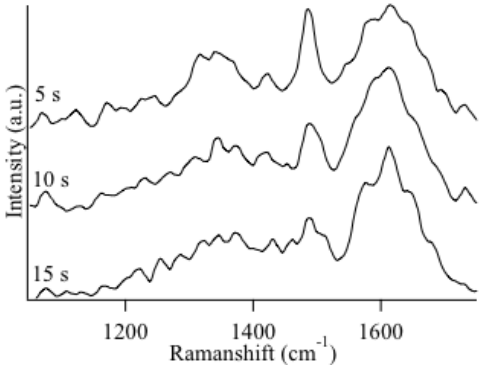

Fig. 4. Raman spectra of live cells in Tyrode's solution for different durations of sample exposure (5, 10, 15 sec). Spectra were smoothed by Loess fitting. Each spectrum is shifted vertically for clear comparison.

Photodamage of live cells in liquid can be affected by the cellular function [26]. Living organisms show four basic responses to stressful radiation, including avoiding, reducing, and acclimating the stress, and repairing the damage due to the stress. These responses can be prevented by fixing the cells by paraformaldehyde. Figure 5(a) shows the Raman spectra of fixed HeLa cells for different exposure durations (5, 10, 15 sec). The decay of the purine base band and the growth of photoproduct in the spectra are apparently confirmed by increasing the exposure duration. Similarly to live cells, the spectrum for the exposure duration of 15 s barely shows the purine base band at 1480 cm^{-1}. This result indicates that cellular functions are not significantly related to the spectral degradation. This is possibly because the cellular responses to DUV, such as molecular repairs and movement away from the radiation, are far slower than the observation duration.

Reactive oxygen species (ROS) play roles in molecular damage in living organisms exposed to DUV [11]. The effect of ROS was examined using the antioxidant agent, Trolox. Figure 5(b) shows the Raman spectra of live HeLa cells with 500 μM Trolox in the Tyrode's bath solution for different exposure durations (5, 10, 15 sec). The quantity of spectral change is essentially the same as that of live cells. This indicates that ROS doesn't play a large role in the molecular degradation observed in DUV Raman spectroscopy, though it should in theory mitigate some of the photodamage processes.

#138099 - $15.00 USD Rec. 12 Nov 2010; revised 18 Feb 2011; accepted 9 Mar 2011; published 18 Mar 2011

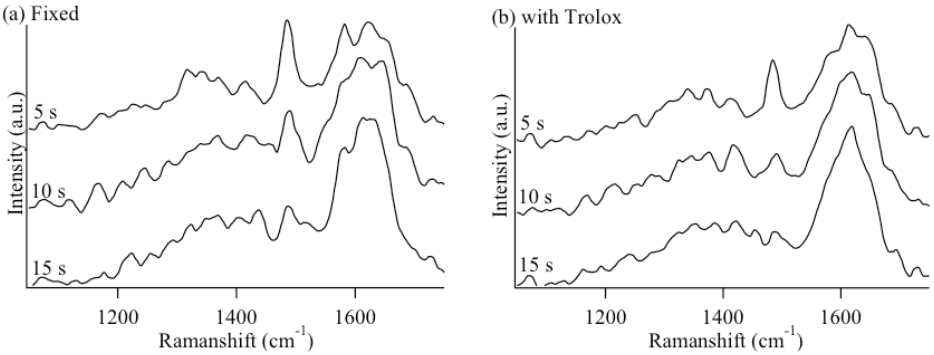

Fig. 5. Raman spectra of (a) fixed cells in Tyrode's solution, (b) live cells in Trolox Tyrode's solution, for different durations of sample exposure (5, 10, 15 sec). Spectra were smoothed by Loess fitting. Each spectrum is shifted vertically for clear comparison.

4. Conclusion

In this study, we applied DUV resonant Raman spectroscopy for characterization of molecular photodegradation in HeLa cells. Raman spectra of cells exposed to Raman excitation light for different durations were measured and analyzed. Spectra obtained from the cells with relatively shorter durations of exposure (0.25~2.5 sec at 16 $\mu W/\mu m^2$) show characteristic Raman bands of aromatic amino acids and nucleotide bases, while longer exposure (7.5~12.5 sec at 16 $\mu W/\mu m^2$) resulted in the disappearance of these bands and the growth of photoproduct bands instead. We used exponential function fitting analyses to quantify the relationship between the exposure durations and Raman intensities of the characteristic bands. As results, the molecular degradation and the photoproduct growth were correlated with the exposure duration. The degradation of purine bases (1483 cm^{-1}) and the growth of photoproduct (1611 cm^{-1}) showed a linear dependence on the number of exposure photons, while the aromatic amino acids showed a nonlinear dependence of molecular degradation on the irradiation intensity. This implies that only the degradation of aromatic amino acids is associated with heating, molecular phototransients, and multi-photon absorption process.

From the obtained fitting curves, the practical maximum exposure energy for DUV Raman observation of cell samples was suggested. The effective energy for the purine bases (1483 cm^{-1}) was 37~41 $\mu J/\mu m^2$. In some cases, the photoproduct became visible before characteristic Raman bands disappeared. The allowable energy for observation without generating significant photoproduct (at 1611 cm^{-1}) was 18~24 $\mu J/\mu m^2$. The effective exposure energy for aromatic amino acids degradation (1618 cm^{-1}) showed a clear dependence on irradiation intensity, in contrast to other bands. 16 $\mu W/\mu m^2$ only allows 1.8 $\mu J/\mu m^2$ exposure, while 1.6 $\mu W/\mu m^2$ allows 18 $\mu J/\mu m^2$, for Raman observation of this band. This work clearly defines the allowable limits for future attempts to create DUV resonant Raman microspectroscopy of individual components in cells excited at or below the allowable maximum energy

Acknowledgments

This work was supported by the Japan Science and Technology (JST) organization via a CREST project and by RIKEN via an Extreme Photonics project. The authors sincerely acknowledge Dr. N. Hayazawa and Dr. A. Tarun of RIKEN Advanced Science Institute for helpful comments on the manuscript and the data analyses.